

# Electrogenerated Chemiluminescence of Donor–Acceptor Molecules with Thermally Activated Delayed Fluorescence\*\*

Ryoichi Ishimatsu,\* Shigeyuki Matsunami, Takashi Kasahara, Jun Mizuno, Tomohiko Edura, Chihaya Adachi,\* Koji Nakano, and Toshihiko Imato\*

**Abstract:** The electrochemistry and electrogenerated chemiluminescence (ECL) of four kinds of electron donor–acceptor molecules exhibiting thermally activated delayed fluorescence (TADF) is presented. TADF molecules can harvest light energy from the lowest triplet state by spin up-conversion to the lowest singlet state because of small energy gap between these states. Intense green to red ECL is emitted from the TADF molecules by applying a square-wave voltage. Remarkably, it is shown that the efficiency of ECL from one of the TADF molecule could reach about 50%, which is comparable to its photoluminescence quantum yield.

Since initial studies on electrogenerated chemiluminescence (ECL) in the 1960s,<sup>[1–3]</sup> many compounds have been synthesized and investigated to attain ECL with higher intensity and efficiency as the operation mechanism of ECL has been clarified. ECL is emitted from an excited species ( $R^*$ ) produced through ion–ion annihilation of a radical anion and cation as a result of an electrochemical reaction.<sup>[4–6]</sup> The ratio of the lowest excited singlet ( $S_1$ ) and triplet ( $T_1$ ) states of  $R^*$  formed by ion–ion annihilation is considered to be 1:3 following spin statistics.<sup>[4,7]</sup> In most fluorescent molecules, the

$T_1$  state cannot contribute to ECL emission because the transition from  $T_1$  to the ground ( $S_0$ ) state is non-radiative. Thus, the maximum ECL efficiency ( $\phi_{\text{ECL}}$ ) is expected to be 25% for most fluorescent materials even if its photoluminescence quantum yield (PLQY) is unity.<sup>[8]</sup>

The limitation of efficiency regulated by spin statistics can be overcome by spin up-conversion induced by thermal activation through reverse intersystem crossing (RISC)<sup>[9]</sup> according to Equation (1):



where  $^3R^*$  and  $^1R^*$  are an excited species at  $T_1$  and  $S_1$ , respectively. A representation of electronic transitions including RISC is shown in Figure 1 a. Because the rate constant for

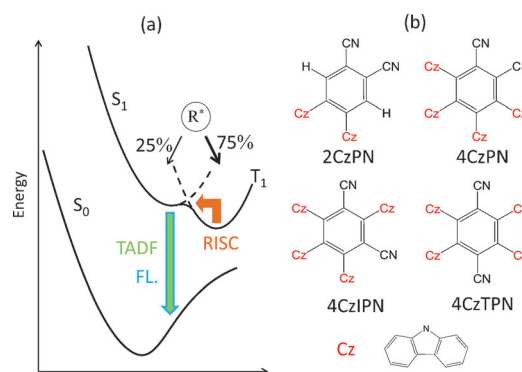


**Figure 1.** a) Representation of electronic transitions and b) molecular structures of the four TADF molecules examined herein.

RISC is much smaller than that for the radiative transition from  $S_1$  to  $S_0$  (the lifetime of fluorescence is in the order of ns), delayed fluorescence (lifetime in the order of  $\mu\text{s}$  to ms) can be observed.<sup>[10]</sup> Efficient thermally activated delayed fluorescence (TADF) can occur when the energy gap between  $S_1$  and  $T_1$  ( $\Delta E_{\text{st}}$ ) is sufficiently small (ca. 0.1 eV).<sup>[11]</sup> Along with a small  $\Delta E_{\text{st}}$ , a high PLQY, that is, large rate constant for the radiative transition from  $S_1$  to  $S_0$ , is needed to achieve a high luminescent efficiency. To satisfy these two requirements, several TADF molecules composed of electron donor(D)–acceptor(A) units with both small  $\Delta E_{\text{st}}$  and high PLQY have been developed recently for application in organic light-emitting diodes (OLEDs).<sup>[10–16]</sup> OLEDs containing TADF materials exhibit excellent performance comparable to those fabricated using phosphorescent materials because of thermal activation of excitons generated by recombination of holes

[\*] Dr. R. Ishimatsu, Prof. C. Adachi, Prof. K. Nakano, Prof. T. Imato  
Department of Applied Chemistry  
Graduate School of Engineering  
Kyushu University (Japan)  
E-mail: Ishimatsu@cstf.kyushu-u.ac.jp  
imato@cstf.kyushu-u.ac.jp

Dr. S. Matsunami, Dr. T. Edura, Prof. C. Adachi  
Center for Organic Photonics and Electronics Research  
Kyushu University  
744 Motooka, Nishi, Fukuoka, 819-0395 (Japan)  
E-mail: adachi@cstf.kyushu-u.ac.jp

T. Kasahara  
Department of Nanoscience and Nanoengineering  
Waseda University  
3-4-1 Okubo, Shinjuku, Tokyo, 169-8555 (Japan)

Prof. J. Mizuno  
Institute for Nanoscience and Nanotechnology  
Waseda University  
513 Wasedatsurumakicho, Shinjuku, Tokyo, 162-0041 (Japan)

[\*\*] This research is supported in part by the Japan Society for the Promotion of Science through its “Funding Program for World-Leading Innovative R&D on Science and Technology”. We acknowledge Hiroshi Miyazaki and Hiroko Nomura (Kyushu University) for the synthesis of TADF molecules. R.I. gratefully acknowledges Prof. Katsumi Tokumaru (Professor Emeritus, University of Tsukuba) for valuable discussion.

Supporting information for this article is available on the WWW under <http://dx.doi.org/10.1002/ange.201402615>.

and electrons. Therefore, TADF molecules are an attractive alternative to phosphorescent materials incorporating transition metals such as Ir and Pt,<sup>[5,17]</sup> which are not abundant. TADF molecules can be used as emitters in the ECL system and are expected to give high ECL efficiency through spin up-conversion from  $T_1$  to  $S_1$ .

In this study, we demonstrate highly efficient green to red ECL using four kinds of TADF molecules,<sup>[14]</sup> 1,2-bis(carbazol-9-yl)-4,5-dicyanobenzene (2CzPN), 1,2,3,4-tetrakis(carbazol-9-yl)-5,6-dicyanobenzene (4CzPN), 1,2,3,5-tetrakis(carbazol-9-yl)-4,6-dicyanobenzene (4CzIPN), and 1,2,4,5-tetrakis(carbazol-9-yl)-3,6-dicyanobenzene (4CzTPN), the structure of which are shown in Figure 1b. Carbazolyl and dicyanobenzene groups behave as an electron donor and acceptor, respectively. We show that the ECL efficiency of these TADF molecules can exceed the limitation followed by the spin statistics (25% of PLQY), and that it is in fact possible to reach to the PLQY.

First, to investigate the electrochemical properties of the four TADF molecules, cyclic voltammetry was carried out employing a conventional three-electrode system using a Pt disk ( $d = 1.6$  mm), a Pt wire, and Ag wire as working, counter, and reference electrodes, respectively.

Cyclic voltammograms of 2CzPN, 4CzPN, and 4CzIPN in acetonitrile (MeCN) solutions containing 0.1 M tetrabutylammonium hexafluorophosphate (TBAPF<sub>6</sub>) as a supporting electrolyte are presented in Figure 2. (A cyclic voltammo-

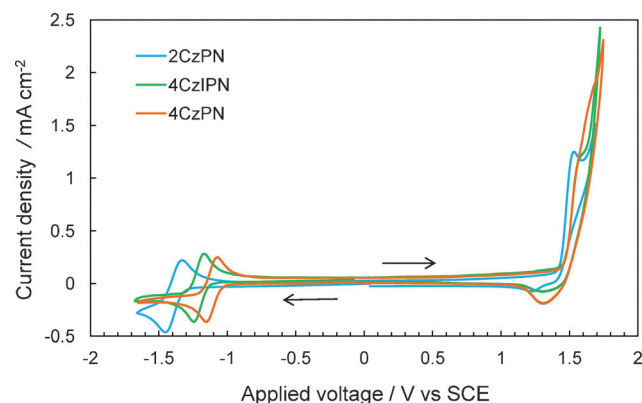


**Figure 2.** Cyclic voltammograms of 1 mM 2CzPN, 4CzPN, and 4CzIPN in MeCN containing 0.1 M TBAPF<sub>6</sub>. Scan rate: 100 mV s<sup>-1</sup>. Arrows indicate scan direction.

gram of 4CzTPN in dichloromethane (DCM) is shown in the Supporting Information, Figure S2 because 4CzTPN hardly dissolved in MeCN). Quasi-reversible waves for reduction of dicyanobenzene group (A) in cathodic scans were observed for the four TADF molecules. By fitting the voltammograms with results of digital simulation, the standard redox potential  $E^0(R/R^-)$  and heterogeneous rate constant  $k^0(R/R^-)$  of the electrode reaction for dicyanobenzene groups were estimated (Supporting Information, Figure S3).  $E^0$  related to the HOMO–LUMO energy gap ( $E_{L-H}$ ) and  $k^0$  affect ECL spectra and the response for ECL, respectively. Table 1 summarizes the electrochemical properties of the TADF molecules with

**Table 1:** Electrochemical properties of TADF molecules.

	$E^0(R/R^-)$ [V] <sup>[b]</sup>	$E_{pa}$ <sup>[a]</sup> [V] <sup>[b]</sup>	$k^0(R/R^-)$ [cm s <sup>-1</sup> ]	$E_{L-H}$ [eV] <sup>[c]</sup>
2CzPN	-1.45	1.47	0.012	3.38
4CzPN	-1.16	N.D.	0.013	3.06
4CzIPN	-1.21	1.52	0.014	3.11
4CzTPN <sup>[d]</sup>	-1.02	N.D.	0.013	2.91

[a] Peak potential in the anodic scan. N.D. = not determined. [b] Potential vs SCE. [c] Calculated by a DFT method. [d] Data measured in 0.4 mM DCM solution.

$E_{L-H}$  calculated by a density functional theory (DFT) method (B3LYP/6-31 + (d) of the optimized structures; Gaussian09).  $E^0(R/R^-)$  for the dicyanobenzene groups (A) depend on the number and location of carbazolyl units (D), which are related to the LUMO level of the TADF molecules. The difference of  $E^0(R/R^-)$  between 2CzPN and 4CzIPN, 4CzPN, and 4CzTPN are 0.24, 0.29, and 0.43 V, respectively. This trend is consistent with the difference of  $E_{L-H}$  of 4CzIPN (0.27 eV), 4CzPN (0.32 eV), and 4CzTPN (0.47 eV) with respect to that of 2CzPN calculated by the DFT method. In contrast,  $k^0(R/R^-)$  for the dicyanobenzene groups of the TADF molecules showed less variation (0.012–0.014 cm s<sup>-1</sup>).

In the anodic scans, irreversible waves corresponding to oxidation of the carbazole groups (D) were observed. The irreversibility is caused by polymerization of TADF molecules and formation of a polymer film on the Pt electrode, as was observed in electrochemical oxidation of carbazole<sup>[18]</sup> and a molecule with carbazolyl moieties.<sup>[19]</sup> Comparing the anodic peak current with the cathodic peak current for the dicyanobenzene groups, two-electron oxidation of the carbazolyl group occurred for 2CzPN and 4CzIPN. For 4CzPN and 4CzTPN, because of unclear peak shape in the cathodic scan, the number of electrons for the oxidation was not able to be determined exactly, but it seems to be two- or three-electron oxidation. Such simultaneous oxidation of carbazolyl groups is caused by torsion between the carbazolyl and dicyanobenzene groups.<sup>[14]</sup>

Solvent polarity is known to affect both the photophysical and ECL properties of materials. Thus, DCM and MeCN, which are commonly used as solvents for electrochemical measurements, were used in the following experiments to reveal the relationship between photophysical and ECL properties of the four kinds of TADF molecules. Figure 3 shows UV/Vis absorbance and photoluminescence (PL) spectra of the TADF molecules in DCM and MeCN. The maximum wavelength of absorption ( $\lambda_{abs}$ ) and PL ( $\lambda_{PL}$ ) are listed in Table 2. The HOMO–LUMO transition observed as the absorption in the UV/Vis range shows charge transfer (CT) characteristics, that is, an electronic transition occurs from carbazolyl to dicyanobenzene groups upon light absorption.<sup>[14,20]</sup>

$\lambda_{abs}$  and  $\lambda_{PL}$  shifted to shorter and longer wavelength, respectively, when the solvent polarity increased from DCM to MeCN, which is typical for D–A molecules with CT characteristics.<sup>[19,21–23]</sup>  $\lambda_{PL}$  appeared at 530–610 nm, and the trend of  $\lambda_{PL}$  is consistent with those of  $E^0(R/R^-)$  and  $E_{L-H}$  determined by the DFT calculation (Table 1).

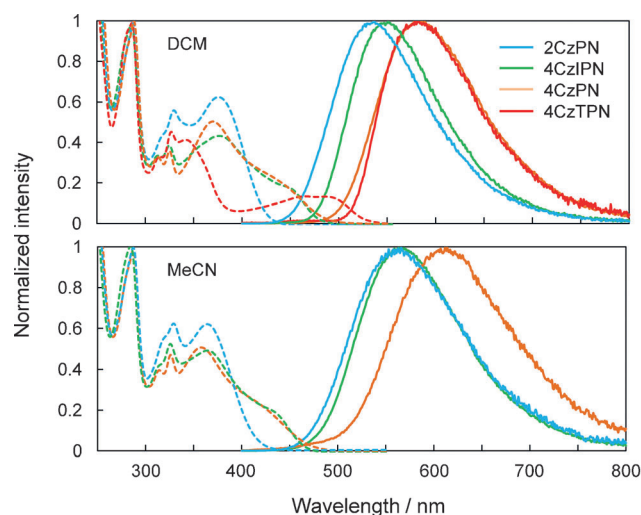


**Figure 3.** Normalized UV/Vis absorption (broken lines) and PL spectra (solid lines) of 25  $\mu\text{M}$  TADF molecules in DCM (top) and MeCN (bottom).

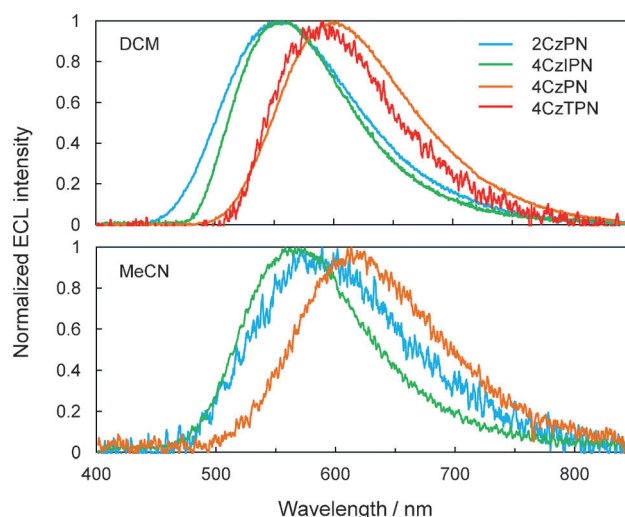


**Figure 4.** Normalized ECL spectra of TADF molecules in DCM (top) and MeCN (bottom).

**Table 2:** Photophysical and ECL properties of TADF molecules.

	Solvent	$\lambda_{\text{abs}}^{[a]}$ [nm]	$\lambda_{\text{PL}}^{[a]}$ [nm]	$\lambda_{\text{ECL}}^{[a]}$ [nm]	PLQY [%]	$\phi_{\text{ECL}}^{[b]}$ [%]
2CzPN	DCM	374	533	550	34	$4.5 \pm 0.6$
	MeCN	367	560	585	10	$1.1 \pm 0.1$
4CzPN	DCM	369	583	595	29	$14 \pm 2.0$
	MeCN	359	609	610	7.5	$2.1 \pm 0.3$
4CzIPN	DCM	379	544	555	54 <sup>[c]</sup>	$47 \pm 6.0$
	MeCN	370	565	565	18 <sup>[c]</sup>	$15 \pm 1.6$
4CzTPN	DCM	492	581	600	15	$6.0 \pm 0.9^{[d]}$

[a] At the longest wavelength. [b] Calculated from integrated ECL intensity at  $\lambda_{\text{ECL}}$  and charge compared with that of the 1 mm or 0.4 mm  $[\text{Ru}(\text{bpy})_3]^{2+}$  system with  $\phi_{\text{ECL}} = 5\%$ . [c] From Ref. [20]. [d] Measured at 0.4 mm.

As discussed above (Figure 2), oxidation of these four TADF molecules initiates polymerization. Although polymerization may inhibit ECL by inactivation of electrodes, it was possible to observe intense ECL by applying a square-wave voltage to generate both radical anion and cation at the Pt disk electrode. The ECL spectra obtained for the TADF molecules with a square-wave voltage (50–100 Hz) in the diffusion-limited region for the electrode reaction are presented in Figure 4. The maximum wavelengths of ECL ( $\lambda_{\text{ECL}}$ ) are summarized in Table 2. As observed in the PL spectra,  $\lambda_{\text{ECL}}$  was red-shifted when the solvent polarity was increased from DCM to MeCN. Furthermore,  $\lambda_{\text{ECL}}$  exhibits a slight red-shift compared with that of  $\lambda_{\text{PL}}$  except for 4CzIPN in MeCN (Table 2). This difference can be partially explained by the presence of the supporting electrolyte. The supporting electrolyte can shift  $\lambda_{\text{PL}}$  to longer wavelength in DCM but not in MeCN solutions (Supporting Information, Figure S7). It is likely that in the excited states, highly polar excitons with CT characteristics interact more with supporting electrolyte ions in a less polar medium. However, for 2CzPN and 4CzPN,  $\lambda_{\text{ECL}}$  shifted by more than would be expected from the effect of the supporting electrolyte alone (Supporting Information,

Figure S8). This can be explained by the emission from oligomers such as dimers and trimers which were formed during oxidation by applying a square-wave voltage.

To estimate the ECL efficiencies of 2CzPN, 4CzPN, 4CzIPN, and 4CzTPN solutions, a train of pulse voltage was applied, which is a convenient method to estimate ECL efficiency.<sup>[4]</sup> Figure 5 shows the ECL intensities of TADF molecules in MeCN and DCM with 1 mM tris(2,2'-bipyridine)ruthenium ( $[\text{Ru}(\text{bpy})_3]^{2+}$ ) as a standard substrate for ECL ( $\phi_{\text{ECL}} = 5\%$  in MeCN because of electron transfer between  $[\text{Ru}(\text{bpy})_3]^{3+}$  and  $[\text{Ru}(\text{bpy})_3]^{2+}$ ,<sup>[24]</sup> and no ECL in DCM because of electrochemical deposition in less polar solvents<sup>[25]</sup>). ECL intensity depended on the solvent polarity; DCM solutions gave higher intensity than MeCN ones, consistent with PLQY values. Remarkably, the maximum

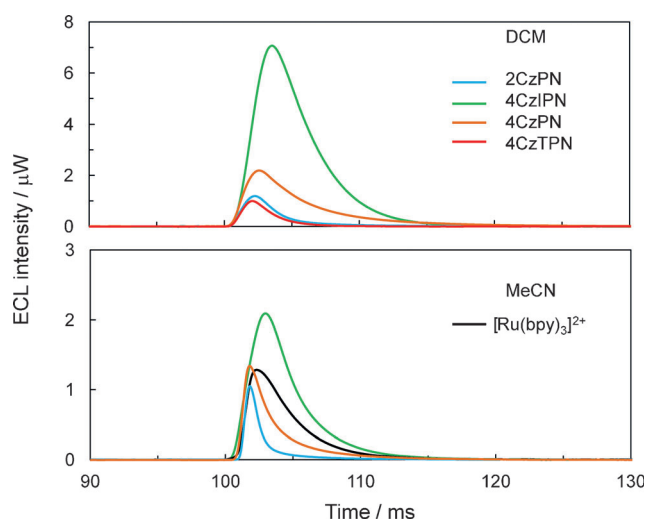


**Figure 5.** ECL intensity of TADF molecules generated by applying a train of pulse voltage (5 Hz) at  $\lambda_{\text{ECL}}$  in DCM (top) and MeCN (bottom). Concentration: 1 mM for 2CzPN, 4CzPN, 4CzIPN, and  $[\text{Ru}(\text{bpy})_3]^{2+}$ , and 0.4 mM for 4CzTPN.

ECL intensities of 4CzIPN solutions were much higher than that of the  $[\text{Ru}(\text{bpy})_3]^{2+}$  system. The estimated  $\phi_{\text{ECL}}$  value from the integration of the ECL intensity and charges during the potential step (Supporting Information) reached about 50% in DCM. As far as we know, this is the most efficient ECL system reported to date using fluorescent molecules and comparable to very efficient ECL systems using phosphorescence materials such as Ir,<sup>[26]</sup> Os,<sup>[27]</sup> and Ru<sup>[28,29]</sup> chelates. Moreover,  $\phi_{\text{ECL}}$  (Table 2) obtained for 4CzIPN exceeded the limitation of spin statistics ( $\phi_{\text{ECL}} = 0.25 \times \text{PLQY}$ ), and was comparable to PLQY. It should be noted that the PL intensity of 4CzIPN decreased by about 15% in the presence of 0.1M TBAPF<sub>6</sub> (Supporting Information, Table S3). Therefore, we conclude that  $\phi_{\text{ECL}}$  is essentially same as PLQY for 4CzIPN. This fact coupled with the agreement of the PL with the ECL spectra confirms that the pathway of both emissions from 4CzIPN is the same, that is, excitons at S<sub>1</sub> and T<sub>1</sub> were generated efficiently by ion annihilation and generated excitons at T<sub>1</sub> were up-converted to S<sub>1</sub> by thermal activation, resulting in delayed ECL.

It is expected that such thermal activation of excitons is also valid for 2CzPN, 4CzPN, and 4CzTPN, and  $\phi_{\text{ECL}}$  correspond to PLQY. 4CzPN in DCM gave relatively large  $\phi_{\text{ECL}}$  (about three times higher than the  $[\text{Ru}(\text{bpy})_3]^{2+}$  system). However,  $\phi_{\text{ECL}}$  for 2CzPN, 4CzPN, and 4CzTPN were smaller than their corresponding PLQY considering the effect of the supporting electrolyte. This decrease in  $\phi_{\text{ECL}}$  is attributed to inefficient emission from the corresponding polymer including oligomers such as dimers and trimers, and inactivation of the Pt electrode by the polymer film. In fact, the ECL intensity of 2CzPN and 4CzPN in MeCN decayed quickly (Figure 5), suggesting that the surface of the electrode was covered with their polymer films during oxidation.

In summary, we demonstrated several TADF molecules that exhibit ECL emission with high efficiency, which can almost reach the corresponding PLQY. This indicates that spin up-conversion through thermal activation is very useful for ECL, and ECL from TADF molecules has great potential to be used in liquid light-emitting devices and ECL immunoassay because of their high ECL efficiency.

Received: February 20, 2014

Published online: May 22, 2014

**Keywords:** electrochemiluminescence · electrochemistry · kinetics · quantum yield · solvent effects

- [2] R. E. Visco, E. A. Chandross, *J. Am. Chem. Soc.* **1964**, *86*, 5350–5351.
- [3] K. S. V. Santhanam, A. J. Bard, *J. Am. Chem. Soc.* **1965**, *87*, 139–140.
- [4] *Electrogenerated Chemiluminescence* (Ed.: A. J. Bard), Dekker, New York, **2004**.
- [5] M. M. Richter, *Chem. Rev.* **2004**, *104*, 3003–3036.
- [6] W. Miao, *Chem. Rev.* **2008**, *108*, 2506–2553.
- [7] N. R. Armstrong, R. M. Wightman, E. M. Gross, *Annu. Rev. Phys. Chem.* **2001**, *52*, 391–422.
- [8] K. M. Maness, R. M. Wightman, *J. Electroanal. Chem.* **1995**, *396*, 85–95.
- [9] a) C. A. Parker, *Photoluminescence of Solutions*, Elsevier, Amsterdam, The Netherlands, **1968**; b) A. Kapturkiewicz, J. Herbich, J. Nowacki, *Chem. Phys. Lett.* **1997**, *275*, 355–362.
- [10] T. Nakagawa, S.-Y. Ku, K.-T. Wong, C. Adachi, *Chem. Commun.* **2012**, *48*, 9580–9582.
- [11] S. Youn Lee, T. Yasuda, H. Nomura, C. Adachi, *Appl. Phys. Lett.* **2012**, *101*, 093306.
- [12] A. Endo, M. Ogasawara, A. Takahashi, D. Yokoyama, Y. Kato, C. Adachi, *Adv. Mater.* **2009**, *21*, 4802–4806.
- [13] Q. Zhang, J. Li, K. Shizu, S. Huang, S. Hirata, H. Miyazaki, C. Adachi, *J. Am. Chem. Soc.* **2012**, *134*, 14706–14709.
- [14] H. Uoyama, K. Goushi, K. Shizu, H. Nomura, C. Adachi, *Nature* **2012**, *492*, 234–238.
- [15] G. Méhes, H. Nomura, Q. Zhang, T. Nakagawa, C. Adachi, *Angew. Chem.* **2012**, *124*, 11473–11477; *Angew. Chem. Int. Ed.* **2012**, *51*, 11311–11315.
- [16] F. B. Dias, K. N. Bourdakos, V. Jankus, K. C. Moss, K. T. Kamtekar, V. Bhalla, J. Santos, M. R. Bryce, A. P. Monkman, *Adv. Mater.* **2013**, *25*, 3707–3714.
- [17] G. Zhou, W.-Y. Wong, X. Yang, *Chem. Asian J.* **2011**, *6*, 1706–1727.
- [18] P. Marrec, C. Dano, N. Gueguen-simonet, J. Simonet, *Synth. Met.* **1997**, *89*, 171–179.
- [19] K. M. Omer, S.-Y. Ku, Y.-C. Chen, K.-T. Wong, A. J. Bard, *J. Am. Chem. Soc.* **2010**, *132*, 10944–10952.
- [20] R. Ishimatsu, S. Matsunami, K. Shizu, C. Adachi, K. Nakano, T. Imato, *J. Phys. Chem. A* **2013**, *117*, 5607–5612.
- [21] J. Suk, J.-Z. Cheng, K.-T. Wong, A. J. Bard, *J. Phys. Chem. C* **2011**, *115*, 14960–14968.
- [22] Y. O. Lee, T. Pradhan, K. Choi, D. H. Choi, J. H. Lee, J. S. Kim, *Tetrahedron* **2013**, *69*, 5908–5912.
- [23] P. Natarajan, M. Schmittel, *J. Org. Chem.* **2013**, *78*, 10383–10394.
- [24] W. L. Wallace, A. J. Bard, *J. Phys. Chem.* **1979**, *83*, 1350–1357.
- [25] K. Winkler, M. E. Płońska, K. Rečko, L. Dobrzyński, *Electrochim. Acta* **2006**, *51*, 4544–4553.
- [26] A. Kapturkiewicz, T.-M. Chen, I. R. Laskar, J. Nowacki, *Electrochem. Commun.* **2004**, *6*, 827–831.
- [27] G. Angulo, A. Kapturkiewicz, S.-Y. Chang, Y. Chi, *Inorg. Chem.* **1991**, *318*, 91–99.
- [28] P. McCord, A. J. Bard, *J. Electroanal. Chem.* **1991**, *318*, 91–99.
- [29] A. Kapturkiewicz, *Chem. Phys. Lett.* **1995**, *236*, 389–394.

[1] D. M. Hercules, *Science* **1964**, *145*, 808–809.